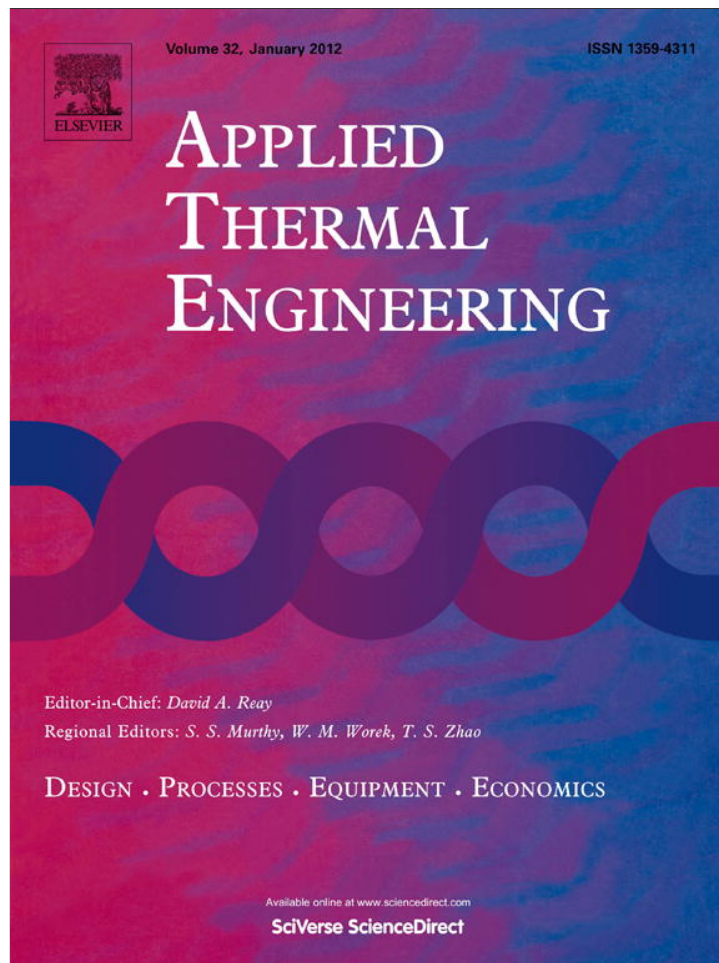


Provided for non-commercial research and education use.
Not for reproduction, distribution or commercial use.



(This is a sample cover image for this issue. The actual cover is not yet available at this time.)

This article appeared in a journal published by Elsevier. The attached copy is furnished to the author for internal non-commercial research and education use, including for instruction at the authors institution and sharing with colleagues.

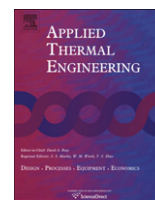
Other uses, including reproduction and distribution, or selling or licensing copies, or posting to personal, institutional or third party websites are prohibited.

In most cases authors are permitted to post their version of the article (e.g. in Word or Tex form) to their personal website or institutional repository. Authors requiring further information regarding Elsevier's archiving and manuscript policies are encouraged to visit:

<http://www.elsevier.com/copyright>

Contents lists available at [SciVerse ScienceDirect](http://www.sciencedirect.com)

Applied Thermal Engineering

journal homepage: www.elsevier.com/locate/apthermeng

New method for designing an effective finned heat exchanger

Diala Karmo^{a,*}, Salman Ajib^b, Ayman Al Khateeb^c^a Institute of Thermodynamics and Fluid Mechanics, Ilmenau University of Technology, Helmholtzring 1, 98693 Ilmenau, Germany^b Department for Environmental Engineering and Applied Informatics, Section Renewable Energies and Decentralized Energy Supplying, Hochschule Ostwestfalen-Lippe, Wilhelmshöhe 44, 37671 Höxter, Germany^c Department for Industrial Engineering, Faculty of Mechanical Engineering, Ilmenau University of Technology, Gustav-Kirchhoff-Platz 2, 98693 Ilmenau, Germany

H I G H L I G H T S

- ▶ We develop a method for designing an effective finned heat exchanger.
- ▶ This new design characterize by smaller dimensions of the heat exchanger.
- ▶ The tubes bend in a zigzag shape. Consequently, the fin block forms a zigzag shape.
- ▶ The new design leads to significant increase in the heat transfer.

A R T I C L E I N F O

Article history:

Received 10 May 2012

Accepted 28 September 2012

Available online 8 October 2012

Keywords:

Zigzag shape

Corrugated fin-tube exchangers

Heat transfer enhancement

Pressure drop

Numerical simulation

CFD

A B S T R A C T

This paper presents a computational analysis of the heat transfer and pressure drop in a finned tube heat exchanger. The main objectives are to develop a method for designing an effective finned heat exchanger through changing the arrangement of the fins and tubes so that the tubes can be bent in a zigzag shape. Thus, they present an angle of less than 90° to the vertical fins. Consequently, the fin block forms a zigzag shape. The construction and the dimensions of the developed alternative heat exchanger are comprehensively presented. This new design is characterized by smaller dimensions of the heat exchanger and allows an increase of the heat transfer on the surface of the fins. Furthermore, a slight increase in the fan and pump power can result, which is very small compared with the recovered heat transfer. However, an effective model is analyzed by means of the computational fluid dynamics (CFD), FLUENT code, which is used to solve the equation for the heat transfer and pressure drop. The major results of the work show an increase in the heat transfer value of 59.13% in comparison to the existing old model. This increase is also accompanied by an increase in the ratio between the total power consumption and the amount of heat transfer obtained of 3.84% compared to 0.8% in the old model.

© 2012 Elsevier Ltd. All rights reserved.

1. Introduction and problem description

Finned tube heat exchangers are widely used in thermal engineering applications. Due to their fins, a large total heat transfer area can be provided. In this case, many studies have been carried out in order to enhance the convective heat transfer of finned tube heat exchangers. Therefore, many investigations into heat transfer performance characteristics of the finned tube exchangers have been experimentally and numerically executed. Most of these focus on the change of the geometrical parameters of tubes and fins and, accordingly, their shape. For example, the diameter of the tubes, their arrangement and forms have been investigated under various

conditions by Kaminski and Groß [1], István [2] and Lu et al. [3]. The effect of the number of tube rows on the efficiency of finned tube heat exchangers has numerically been investigated by Kaminski [4]. He showed that increasing the number of tube rows causes a decrease in the heat transfer coefficient and an increase in the pressure drop. Remero-Mendez et al. [5] and Liu et al. [6] have analyzed the effects of the fin pitch on the heat transfer and the pressure drop. Kim et al. [7] have conducted experimental investigations into the effects of fin type and fin and tube alignment on the heat transfer performance. They have shown that the heat transfer performance can be improved by 20% by applying both the staggered fin and tube alignments in comparison to the continuous flat plate finned tube. Different tube arrangements with plain and corrugated fins have been investigated by Abu Madi et al. [8] both experimentally and numerically. They showed that corrugated fins entail a better heat transfer and a higher friction factor due to their

* Corresponding author. Tel.: +49 3677 69 2414; fax: +49 3677 69 2411.
E-mail address: diala.karmo@tu-ilmenau.de (D. Karmo).

Nomenclature

\dot{Q}	heat transfer rate, W
T	temperature, K
K	thermal conductivity, W/m K
u	velocity, m/s
C_p	specific heat capacity, J/kg K
ρ	density for an incompressible fluid, kg/m ³
μ	dynamic viscosity, kg/s m
φ	conserved quantity per unit mass
S_φ	volumetric source term, with units of conserved quantity per unit volume per unit time
Γ_φ	kinematic diffusivity for the scalar
\dot{V}	volumetric flow rate, m ³ /s
\dot{m}	mass flow rate, kg/s
$\Delta p, p$	pressure drop and pressure, N/m ²
P	loss power associated with pressure drop, W
η	the effectiveness of the fan or pump
$\theta^\circ, \beta^\circ$	inclined fin and tube angle
α°	angle of elbow of the tubes
A	heat transfer surface area, m ²
ΔT	inlet and outlet temperature difference of the air, K

transfer and pressure drop values have been analyzed with inclined fins at different angles (0°, 5°, 10°, 15°, 20°, 25° and 30°). It has been shown that the inclination of the fins at different angles has a substantial effect on the increase in heat transfer. Hence, an increase in the inclination angles of the fins causes a decrease in the distance between adjacent fins, which increases the flow velocity on the cross-section areas between the fins. Furthermore, the contact area between the fins and tubes is increased. In return, this leads to an enhancement of the heat transfer values. Since the increase in the fin angle causes a reduction of the dimensions of the heat exchanger, an inclination angle of 30° was determined to be optimal. Karmo and Ajib [14] have studied the influence exerted by a change of the shape and inclination of the fins on heat transfer. It has been shown that increasing both the area and the inclination of the fins at the same time leads to the largest gain in the heat transfer values. The more the fin angle is increased, the more the heat transfer and also the pressure drop increase.

Because the fin inclination leads to a considerable improvement in heat transfer without any additional investment costs, we will concentrate on the two previous studies. Also, the disadvantages must be investigated and eliminated as far as possible. To keep the dimensions of the heat exchanger constant, the fin number must be reduced by increasing the inclination of the fins. To better illustrate this disadvantage, a graphical comparison between two arrays of fins and tubes is illustrated in Fig. 1. It is assumed that the heat exchanger consists of only one tube row as in Ref. [13]. Fig. 1b shows that a part of the tube with mean length ($j/2$) at the two sides of the tube cannot be covered with fins any more. This means that the length of the uncovered tube part is ($2 \cdot j/2$). This value equals the fin height H multiplied by $\sin \theta^\circ$.

$$j = H \cdot \sin \theta^\circ \tag{1}$$

The more the fin angle increases, the longer the non-covered tube part is, and, therefore, heat transfer is lower in the heat exchanger. Assuming that the heat exchanger consists of more than one tube row, this could mean that the inclination of fins is no longer plausible because of the long non-covered tube part, which depends on the length and on the inclination of the fins. In order to enable an economical inclination of the fins in heat exchangers with more tube rows, it is necessary to develop an approach for providing a new arrangement of the fins and the tubes in heat

higher turbulence. Tsai and Jang [9] have investigated numerically the fin and tube heat exchanger with louver fin. They have used the louver angle of the fin as optimizer to achieve the maximum performance of the heat exchanger. In addition, a literature survey of publications which addressed different types of arrangements of fins was presented in Ref. [10]. Furthermore, Ghiani [11] has developed a flat tube heat exchanger for the use in motor vehicles. The heat transfer increases due to the enlarged surfaces of the tubes by bending the flat tubes in a zigzag shape. Pasha [12] has investigated the heat transfer and the pressure drop for a bank of inclined flat tubes. The angle of inclination varied from 0° to 90°. The heat transfer and pressure drop values were considerably increased within the range from 20° to about 80° while both values were slightly increased at the angles smaller than 20° and greater than 80°. Sahin et al. [13] have investigated a commercial heat exchanger with plain fins by performing a three-dimensional, steady-state, laminar flow system numerically. Both the heat

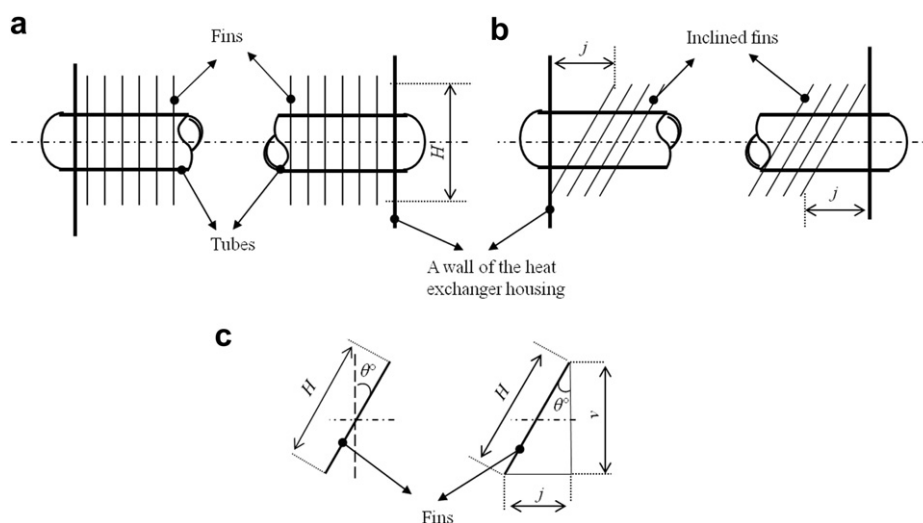


Fig. 1. Representation of the influence of the inclination angle of fins on their number; (a) fins and tube perpendicular to each other, (b) heat exchanger with inclined fins, (c) representation of the tube part, which cannot be covered with fins.

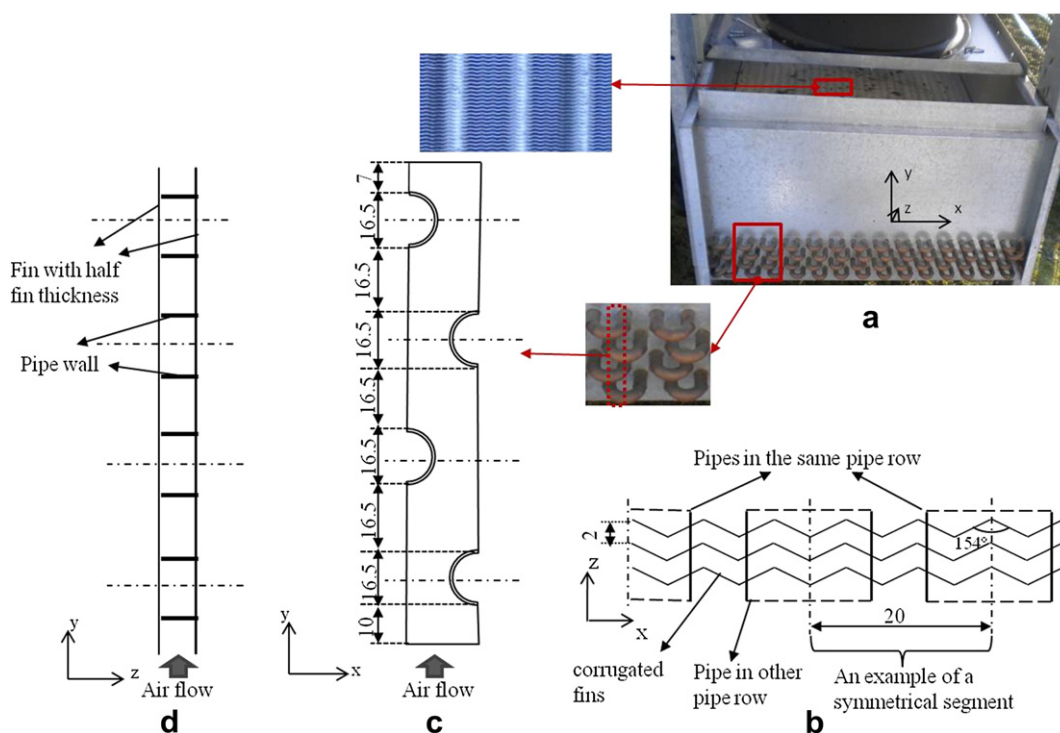


Fig. 2. Illustration of the model studied (all dimensions in mm); (a) front view of the cooling tower, (b) cutaway view of the tubes and fins, (c) dimensions of the analysis model, (d) cutaway view of the analysis model.

exchangers. In this case, the advantages of the fin inclination in the heat exchanger with one tube row must be kept, and the disadvantages mentioned above should be eliminated.

This study focuses on changing the overall arrangement by inclining the tubes rather than the fins. The simulation data are taken from the heat exchanger available in the laboratory of the Institute of Thermodynamics and Fluid Mechanics at Ilmenau University of Technology. The main objective is to develop a method to make the heat exchanger more effective.

2. Description of the heat exchanger investigated and an investigation plan

We will examine a heat exchanger in a dry cooling tower. This cooling tower is connected with an absorption chiller and cools the cooling water for the condenser and the absorber of the absorption chiller. The heat exchanger consists of four rows of round tubes made of copper which are covered with 750 corrugated parallel fins made of aluminum (cf. Fig. 2b). These fins are arranged perpendicular to the tube. The fins are corrugated at an angle of 154°. The thickness of the fins is 0.14 and the space between them is 2 mm. The outer tube diameter is 16.5 mm with a thickness of 0.75 mm. Fig. 2a shows a photograph of the dry cooling tower profile in the laboratory which was measured experimentally by Ajib and Günther [15]. They have investigated the influence of the velocities and temperatures of the cooling water and air on the performance of the cooling tower under different operating conditions. Fig. 2c and d shows the studied model of one segment out of sixty, which was selected because of the symmetry. In general, the model studied consists of two adjacent fins, each of them having half the thickness, and four row staggered tubes. Water flows into the tubes, and air between the fins.

The above-mentioned heat exchanger is modeled and simulated. The heat transfer and pressure drop values obtained from this

model are used as a reference for further comparisons. In order to improve the existing system, two simulation series have been carried out. The first series of simulations have investigated the effects of the inclination of the fins on the heat transfer and pressure drop values. The second series of simulations have tested the heat transfer distribution on the fins and tubes surfaces. The results obtained from these two simulation series have been analyzed, evaluated and have led to a new arrangement of the fins and the tubes. The next step is to describe the new design in general. Different design alternatives can be achieved by varying the influencing parameters. Finally, two alternative designs have been described and analyzed by using the simulation. A comparison of the simulation results with the reference model will be presented.

3. Numerical simulation method

3.1. The mathematical modeling and calculation procedure

The governing equations for three-dimensional continuity, Navier–Stokes for momentum, energy, and scalar transport equations for steady-state flow can be written as follows (cf. [16]).

The continuity equation:

$$\frac{\partial}{\partial x_i} (\rho \cdot u_i) = 0 \quad (2)$$

The momentum equation:

$$\frac{\partial}{\partial x_i} (\rho \cdot u_i \cdot u_j) = \frac{\partial}{\partial x_i} \left(\mu \cdot \frac{\partial u_j}{\partial x_i} \right) - \frac{\partial p}{\partial x_j} \quad (3)$$

The energy equation:

$$\frac{\partial}{\partial x_i} (\rho \cdot u_i \cdot T) = \frac{\partial}{\partial x_i} \left(\frac{k}{c_p} \cdot \frac{\partial u_j}{\partial x_i} \right) \quad (4)$$

General transport equation:

$$\frac{\partial}{\partial x_i} (\rho \cdot u_i \cdot \varphi) = \frac{\partial}{\partial x_i} \left[\Gamma_\varphi \cdot \frac{\partial \varphi}{\partial x_i} \right] + S_\varphi \quad (5)$$

3.2. Boundary conditions

The boundary conditions used in the present study with reference to Fig. 3b were defined as follows:

- The air enters from the bottom surface between two fins (y direction), at a constant velocity of 2 m/s and constant temperature of 298 K.
- The air flows out at the top surface between two fins. So, the outflow boundary condition is given to this surface.
- Symmetrical boundary conditions have been applied to the outer, left and right sides of the model due to the symmetry.
- Wall boundary conditions were used for the inner sides of the tubes, the lower and upper sides of the fins. The convection coefficient between the water flowing inside the tube and the inner wall are calculated according to Gnielinski correlation for turbulent forced convection (cf. Özisik [17], Kakac [18]). Moreover, free stream temperature of the water was assumed to be constant as 311 K.
- The Renormalization Group (RNG) technique with Standard Wall Functions was adopted to simulate turbulence.
- A simplified incompressible flow is used while the compressibility effects will be small due to the small air velocity with a Mach number $< 10^{-2}$ (cf. [19]).
- The physical properties of air and water are constant without the presence of a sharp temperature gradient (cf. [19]).

Because of the complexity of the geometry, quadrilateral mesh elements and an unstructured meshing scheme were applied near the tubes in order to refine it, where the largest variation of the thermal and fluid dynamic variables appears. The model drawn up was created and meshed by using grid generation package of FLUENT, GAMBIT. The grid is illustrated in Fig. 3a.

3.3. Preliminary simulation investigations

A particular challenge in the design to be developed is not to increase the outer dimensions of the heat exchanger. Therefore some preliminary simulation investigations need to be carried out, which help us to find a key to designing an effective heat exchanger. These simulation investigations will be based on the examination of heat transfer and pressure drop values at well-defined fin angles, and also on an examination of the effectiveness of the fins.

3.3.1. Examination of the inclination of the fins

Increasing the inclination angle of the fin in the heat exchanger having a single tube row can mean that the fins cannot cover the tube any more. Since the finned tube heat exchanger is composed of four row staggered tubes as shown in the study of Karmo and Ajib [14], this problem was avoided by reducing the vertical distances between the tube axes. While these distances can be reduced according to the inclination of the fins, the tube axes pierce the fin surfaces at the same positions – as before the inclination operation (at $\theta = 0^\circ$) (see Fig. 4b). Referring to Fig. 4b, these distances were reduced by multiplying the original value (at $\theta = 0^\circ$) with the cosine of an inclination angle of the fin. This means, the vertical distance between the tube axes has changed whereas the height of the fins in between remains constant.

We examine the influence of the change in the inclination angle ($\theta = 0^\circ, 30^\circ, 45^\circ$ and 60°) on heat transfer and pressure drop in the model described in Fig. 2. The simulation results are presented in Table 1.

3.3.2. Examination of heat transfer on the fin sections

It is also known that the heat transfer driving temperature gradient between the surfaces of the fin and fluid decreases continuously with increasing the fin height due to good thermal conductivity of the material of fins [20]. That means the heat transfer values are reduced constantly with increasing the distance from the entrance surface of the gas flowing into the heat exchanger. Therefore we have divided the model described in Fig. 2c and d into four fictitious parts to determine the heat transfer

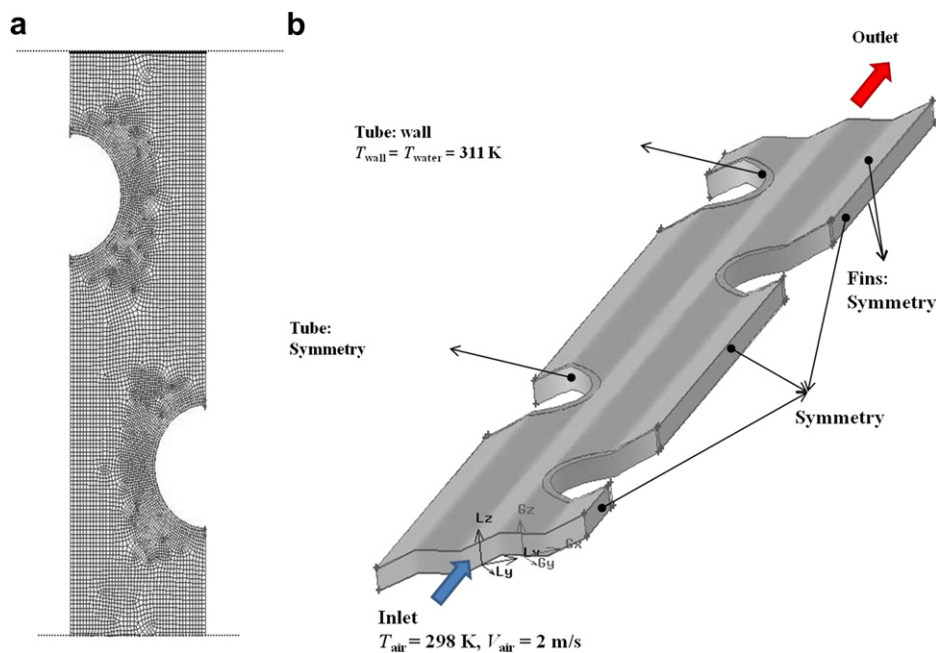


Fig. 3. Illustration of mesh and boundary conditions; (a) mesh configuration, (b) boundary condition.

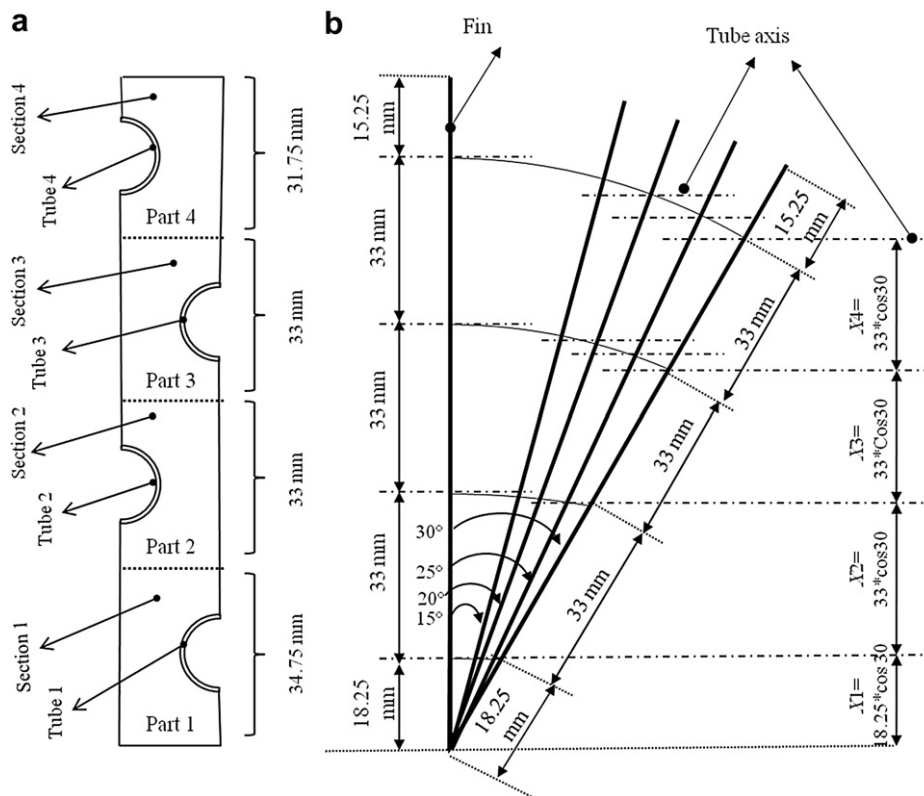


Fig. 4. (a) Division of the investigated model in four parts and the fin piece in four sections. (b) Change of the distances between the tubes as a function of the change in the angle of inclination.

values on the surface of each tube and in the surrounding area of the fin accurately (see Fig. 4a). As an example, we examine the distribution of the heat transfer values for two cases: $\theta = 0^\circ$ and 45° . It is to be considered that in the heat exchanger design tested, the distance between the lower side of the fins and the tube in the lower row (the side of the entry of air) is greater than the distance between the upper side of the fins and the tube in the upper row, where air comes out. For this reason, the fin piece will be divided into four sections 1–4, with sections having a height of 34.75, 33, 33 and 31.75 mm, respectively. To illustrate that, the fictional part 1 consists of a fin section 1 and tube1, whereas the fin section 2 and tube2 belong to fictional part 2, etc. The simulation results are presented in Tables 2 and 3.

3.4. Discussion

The FLUENT was run for each case to obtain heat transfer on the surface of the fins (\dot{Q}_1) and tubes (\dot{Q}_2). Table 1 shows the heat transfer values for the inclination angles of the fin of $\theta = 0^\circ, 30^\circ, 45^\circ, 60^\circ$. Using the pressure drop value ΔP (N/m^2), which is determined numerically, we can calculate the loss power of the fan by means of the following formula (cf. [21]):

$$p = \Delta p \cdot \dot{V} / \eta; \quad (6)$$

We can derive the volumetric flow rate (\dot{V}) from:

$$\dot{V} = \dot{m} / \rho.$$

However, the heat transfer values were normalized to compare the results in all cases. The values of fan power losses were calculated and presented in Table 1. It can be seen that in comparison to $\theta = 0^\circ$, the heat transfer enhancement value for an inclination angle of $\theta = 60^\circ$ was 0.133 W while the normalized value was 113.13%. These results are in good agreement with previous work [13]. It should be noted that the tested tubes have an elliptical shape whereas in our study the tubes are round. However, if the fins are inclined to the tubes, the contact area between the tubes and fins forms an elliptical shape. The emergence of this ellipse contact is considered an important cause for the increase in heat transfer, because of the reduction of the backflow in the wake regions behind the tubes [22]. It has been proven that the high temperature in these regions for elliptical tubes is less than for round tubes.

The maximum loss power associated with the pressure drop per segment at this inclined fin angle was about 0.053 W. The pressure drop increases at a large inclination angle considerably.

Table 1
Comparison of the models at different inclination angles.

Model (θ)	Heat transfer rate (analysis model) $\dot{Q} = \dot{Q}_1 + \dot{Q}_2$ (W)	Heat transfer enhancement in comparison to $\theta = 0^\circ$ (W)	Normalized \dot{Q} (%)	Loss power due to pressure drop $P = \Delta P \cdot \dot{V} / \eta$ (W)	Increase in loss power in comparison to $\theta = 0^\circ$ (W)
0°	1.013	0	100	0.0073	0
30°	1.045	0.032	103.16	0.0113	0.0004
45°	1.086	0.073	107.20	0.020	0.0127
60°	1.146	0.133	113.13	0.060	0.0527

Table 2
Distribution of the heat transfer values in the model studied at an angle of $\theta = 0^\circ$.

Heat transfer rate (W) on the surface of								
Section 1	Section 2	Section 3	Section 4	Tube 1	Tube 2	Tube 3	Tube 4	Sum of the heat transfer (W)
0.4231	0.2567	0.1731	0.1129	0.0188	0.0147	0.0079	0.0054	1.013
Percentage share of total heat transfer rate (%)								
41.77	25.3	17.1	11.15	1.86	1.45	0.78	0.53	≈ 100

Tables 2 and 3 show the detailed heat transfer values on the sections of the fin and the tubes with inclined fin angles $\theta = 0^\circ$ and 45° . Looking at the heat transfer values on the four fictitious parts (1, 2, 3, and 4) of the analysis model (see Fig. 4a), we see that the heat transfer across the surfaces in the fictitious part 1 is the highest compared with those in the fictitious parts 2, 3 and 4. The sum of the percentages of the heat transfer values on the fin sections (1, 2) and on the tubes (1, 2) is about 70% at $\alpha^\circ = 0^\circ$ and about 74% at $\alpha^\circ = 45^\circ$. It can be seen that in Table 3, in comparison with Table 2, the enlargement of the fin inclination increases the heat transfer ratio on the surfaces of those fins and tubes which are closest to the air entrance, and simultaneously, reduces these ratios on the other parts, particularly those which are closest to the air exit. Fig. 5 shows the temperature distribution on the surfaces of the fins by the inclination angle ($\theta = 0^\circ, 30^\circ, 45^\circ$ and 60°).

4. Development of a model for designing an effective heat exchanger

Depending on the above-mentioned results and facts, we try to find an approach to increase the effective area of the fin surface which is closest to the air entrance and simultaneously to reduce the surface of the upper part of the fin. However, the material consumption must not be increased.

Furthermore, the design of the developed model must take into account the following:

- The number of the fins can be increased.
- The height of the fins must be reduced.
- The tube length can be reduced.
- The number of tube rows can be reduced.
- The angle between the fins and tubes must not be 90° .
- The dimensions of the heat exchanger remain constant or can be reduced.

We will design a new model by taking the above-mentioned restrictions into consideration. This can be realized when the tubes are inclined and the fins remain vertically so that the tube pieces are tilted at an angle (β°). They form together several arcs or elbows. Furthermore, tube axes pierce the surfaces of the fins at the same positions as in the case with no inclination of fins or tubes (see Fig. 6). Therefore, the tubes and also the heat exchanger form a zigzag shape.

Table 3
Distribution of the heat transfer values on the studied model at an angle $\theta = 45^\circ$.

Heat transfer rate (W) on the surface of								
Section 1	Section 2	Section 3	Section 4	Tube 1	Tube 2	Tube 3	Tube 4	Sum of the heat transfer (W)
0.493	0.277	0.1714	0.1012	0.0195	0.0131	0.0063	0.004	1.086
Percentage share of total heat transfer rate (%)								
45.4	25.5	15.8	9.3	1.8	1.21	0.58	0.37	≈ 100

Although this paper focuses only on simulation studies, we will try to present a method of mounting fins and tubes below. Both difficulties and facilitations can occur. In the following we will present some of these. It is normal in the manufacturing process to seek for the standard and easy methods that can be applied in the mass production without any difficulty. We should think of such a standard and easy to apply method for the tube-fin joints. Our proposed methods are similar to [11]; soldering and/or pressing. As shown in Fig. 6b, the inclination of the tube will change at different sections from straight to curved tube. Depending on the tube section and the place where the fin will be seated, the contact line between the tubes and fins will change. In those sections where the tubes are straight, the angle between the tube axis and the vertical fin plate will always remain the same and, therefore, the contact line between the tubes and the fins will keep the same elliptical shape. It is easy to apply soldering methods in these sections. In the curved sections the angle between the tube axis and the vertical fin plate increases and decreases steadily, which corresponds to the change of a contact line shape from elliptical to circular and vice versa. In this series of changes the major of the ellipse will decrease until the major and the minor in the tip of curved tubes become equal and the contact line becomes circular. We are supposed to use another manufacturing method for these sections. In order to complete the design based on manufacturing, the model developed has been provided with two types of fins (see Fig. 6c and d). The difference between the fin types is not the fin dimensions but the shape of the holes.

The fins described in Fig. 6c which are suitable for the tubes of the straight sections can be mounted using the soldering techniques. The fins presented in Fig. 6d are meant to be used in the curve sections. They will be applied around the tubes and the slots provided will help to facilitate the mounting of the tubes and fins by the mechanical pressing of the slot against the tube surface.

The conversion into such a zigzag shape can lead to an increase in the height of the heat exchanger and tube length. However, this can be avoided by reducing the fin height, and at the same time, the number of tube rows. Also, the facilitation by manufacturing occurs in reducing the tube rows so that the number of windings outside the heat exchanger tubes is significantly less in comparison to the heat exchanger investigated.

In order to determine the required dimensions for the design of the new model and then to perform a plausible comparison between the new and the old models, we assume that tube length and the dimensions of the heat exchanger remain constant in both

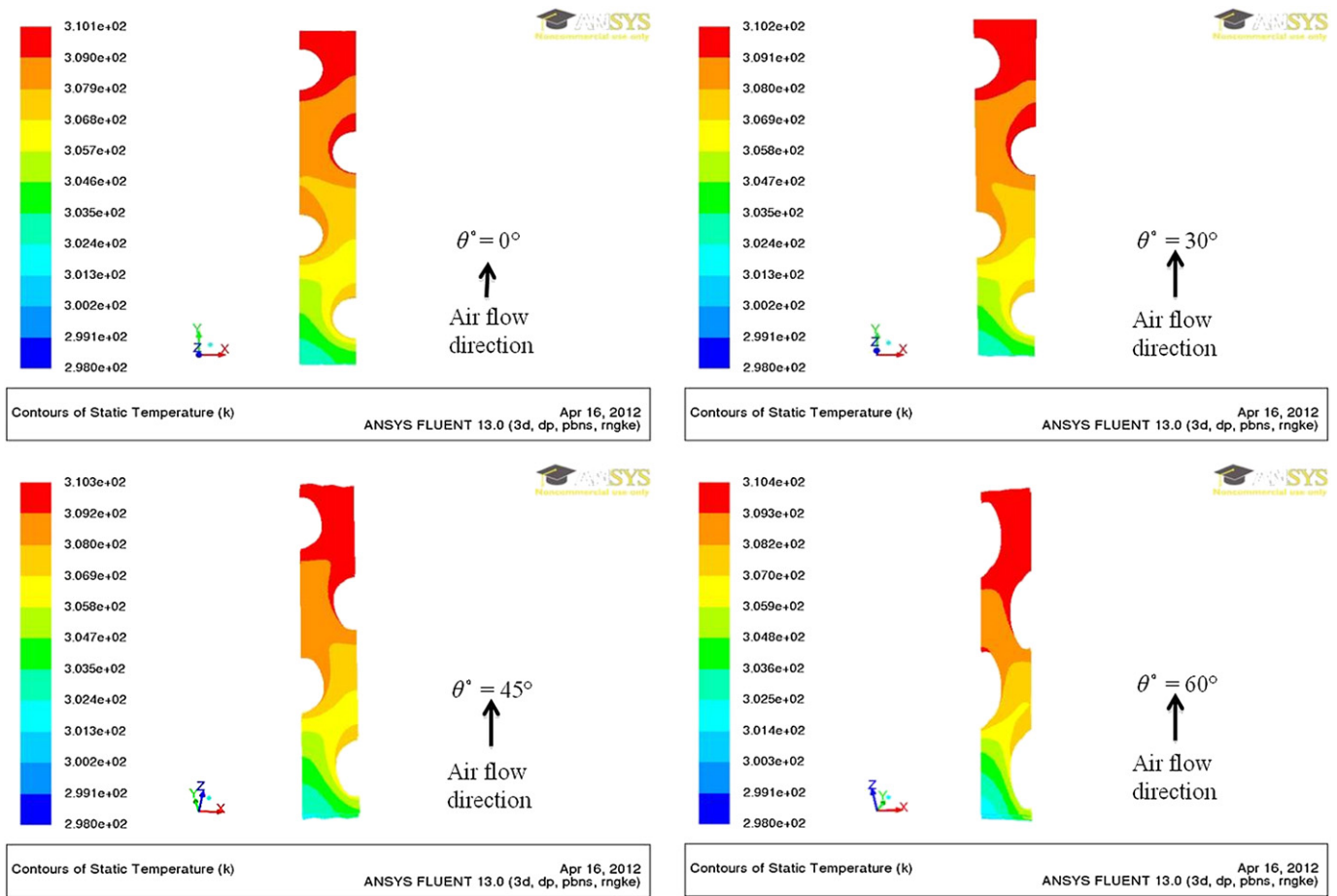


Fig. 5. Temperature distribution on the surfaces of the fins.

cases. By observing the assumptions made above, we will calculate the other dimensions: angle β° , lengths K , M and L (see Fig. 7). To perform this calculation, some formulas will generally be developed.

The height of the heat exchanger Y in the old model is

$$Y = A + B + n \cdot D + (n - 1) \cdot C \quad (7)$$

where A : distance between the lower side of the fin and the lower tube (towards air entrance), B : distance between the top side of the fins and upper tube in the model, C : distance between two adjacent staggered tubes, D : outer tube diameter n : number of tube rows in the old model

The height of the heat exchanger Y_1 in the new model is considered as:

$$Y_1 = A + B + n_1 \cdot D + (n_1 - 1) \cdot C + (n_1 - 1) \cdot K, \quad (8)$$

where: n_1 : number of the tube rows in the new model. K : height of the isosceles triangle (fgh) (see Figs. 6b and 7)

According to the assumptions that the heat exchanger height in both models is the same ($Y = Y_1$) and the parameters A , B , C , D , n , n_1 are known, we can calculate the length K :

$$K = (n - n_1) \cdot (D + C) / (n_1 - 1) \quad (9)$$

In the isosceles triangle in Fig. 7, the following formulas can be written:

$$\sin \alpha^\circ = M / (2L) \quad (10)$$

$$\tan \alpha^\circ = M / (2K) \quad (11)$$

From formulas (9) and (11), the length K is defined as:

$$K = (n - n_1) \cdot (D + C) / (n_1 - 1) = M / (2 \tan \alpha^\circ) \rightarrow \quad (12)$$

Then:

$$M = (2 \tan \alpha^\circ) \cdot (n - n_1) \cdot (D + C) / (n_1 - 1) \quad (13)$$

The length of each staggered tube is regarded as the length of the tube part covered with fins (nearly equal to the length of the heat exchanger), which can be divided into a number of cells (e). Each cell defines the length M in the old model and the length ($2L$) in the new model.

The length Z in the old model is calculated by:

$$Z = M \cdot n \cdot e \quad (14)$$

In the model developed, Z_1 is considered as:

$$Z_1 = (2L) \cdot n_1 \cdot e \quad (15)$$

Assuming that the length Z and e in the old and new model are the same, we can write:

$$M \cdot n \cdot e = (2L) \cdot n_1 \cdot e \rightarrow L = n \cdot M / (2 \cdot n_1) \quad (16)$$

By combining the above formulas (10) and (16), the following relation results:

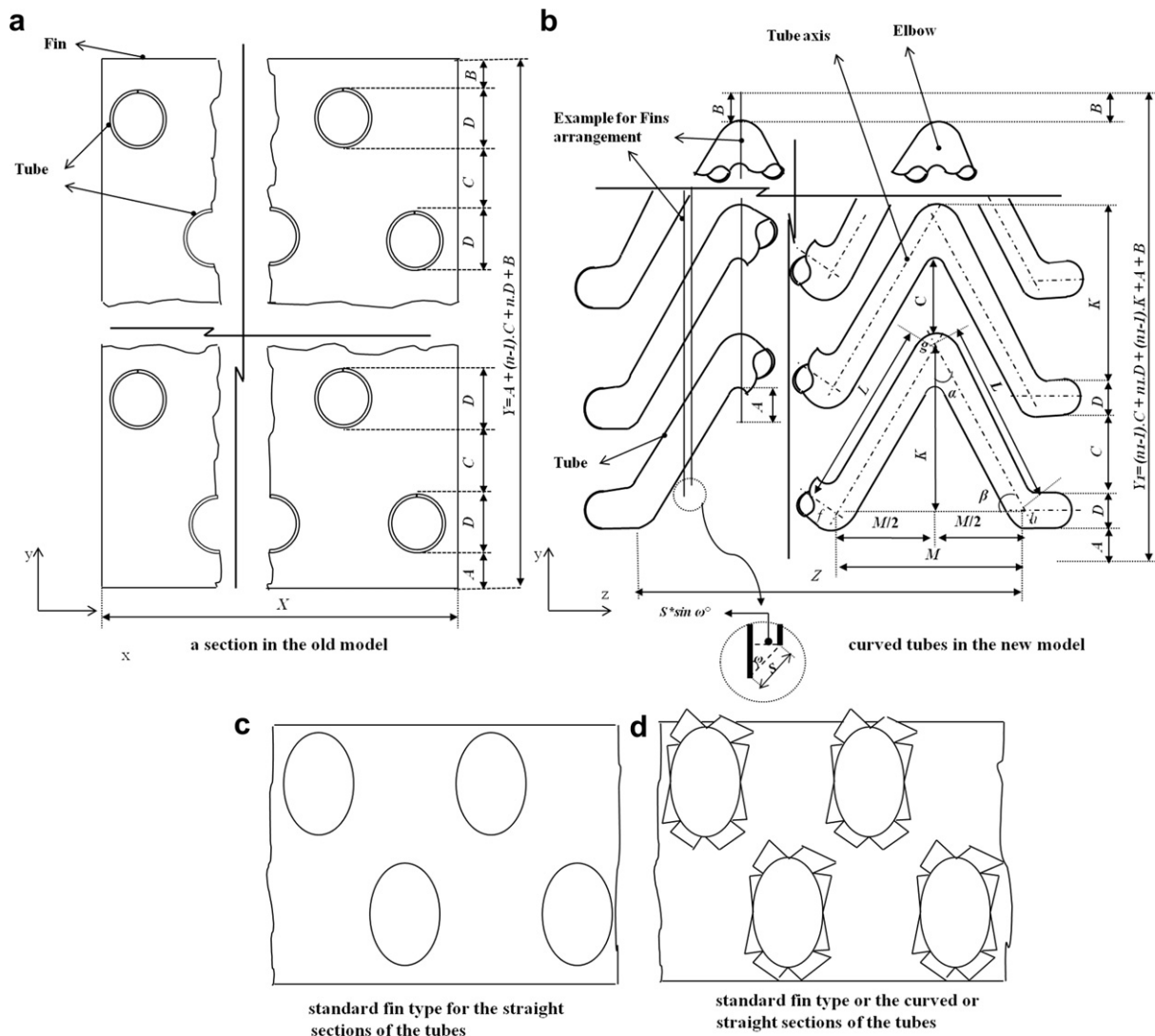


Fig. 6. Some dimensions and sections in old and new models.

$$L = n \cdot M / (2 \cdot n_1) = M / (2 \cdot \sin \alpha^\circ) \rightarrow \sin \alpha^\circ = n / n_1 \quad (17)$$

According to these formulas, it is sufficient to know the number of the tube rows in the old and the new model to calculate the dimensions of any model with this new design. Since the number of fins depends on the length Z , fin thickness t and the distance between the fins, the determination of the maximum number of the fins will be another challenge. By multiplying the number of

fins and the area of just one fin the surface area of the fins can be calculated. In the following studies we will investigate the effects of fin thickness on the number of fins and the amount of fin material used. This will be done through neglecting the thickness of the fins in one case and comparing the results with the real case.

Assuming that the distance between two adjacent fins can be calculated by the formula $(S \cdot \sin \omega^\circ)$, in the special case $\omega^\circ = \alpha^\circ$, it follows that this distance is:

$$S \cdot \sin \omega^\circ = S \cdot \sin \alpha^\circ = S \cdot \cos \beta^\circ \quad (18)$$

We can derive that a part of the heat exchanger with the length (Z_t) is not covered with fins, whereas the fin thickness is not negligible. Taking into account the lengths Z and Z_t are equal, this length value is:

$$Z_t = Z_t - [i_t \cdot (S \cdot \cos \beta^\circ) + i_t \cdot t] = Z_t - i_t \cdot (S \cdot \cos \beta^\circ + t) \quad (19)$$

If in an area of the heat exchanger defined by the length Z , (i_t —fins number) is arranged, the number of fins (i_t') in the field with the length (Z_t') would be defined so that:

$$i_t = (Z_t - S) / (t + S); i_t = 750: \text{The number of fins in the old model}$$

$$i_t' = (Z_t' - S \cdot \cos \beta^\circ) / (t + S \cdot \cos \beta^\circ) \quad (20)$$

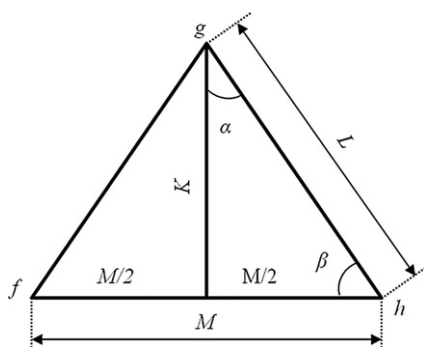


Fig. 7. The isosceles triangle shown in Fig. 6.

i_t' : is the possible increased number of fins, if Z remains the same as in the old model, and the distance between two adjacent fins is $S \cdot \cos \beta^\circ$.

Therefore the total number of fins i_t^s in the new model is obtained:

$$i_t^s = i_t + i_t' = (Z_t - S \cdot \cos \beta^\circ) / (t + S \cdot \cos \beta^\circ) \quad (21)$$

We assume that every fin piece is divided into equal sections. On the one hand, the reduction of the fin height depends on the value of the angle β° ($\cos \beta^\circ = n_1/n$) so that the reduced fin areas P for i_t' -fins number are:

$$P_t = i_t \cdot X \cdot Y (1 - n_1/n) = (Z_t - S) / (t + S) \cdot X \cdot Y \cdot (1 - \cos \beta^\circ) \quad (22)$$

On the other hand, the possible increased fin areas (P_t') for i_t' -fins number are:

$$P_t' = i_t' \cdot X \cdot Y (n_1/n) = (Z_t' - S \cdot \cos \beta^\circ) / (t + S \cdot \cos \beta^\circ) \cdot X \cdot Y \cdot (\cos \beta^\circ) \quad (23)$$

Using formulas (22) and (23) the material consumption of the fins can be calculated. Then we can compare the results of the new with those of the old model.

Furthermore, in an extreme case we assume that the fin thickness is so small that it can be neglected. Hence, the length $Z_{t=0}$ can be calculated by the formula:

$$\begin{aligned} i_{t=0} &= Z_{t=0} / S; \\ i_{t=0} &= i_t = 750 \text{ fins, } Z_{t=0} = i_{t=0} \cdot S = 750 \cdot 2 = 1500 \text{ mm} \end{aligned} \quad (24)$$

Due to the reduction of the distances between the fins results a tube section uncovered with length $Z_{t=0}'$:

$$Z_{t=0}' = Z_{t=0} - Z_{t=0} \cdot \cos \beta^\circ = Z_{t=0} \cdot (1 - \cos \beta^\circ) \quad (25)$$

So the number of fins in the new models becomes:

$$i_{t=0}' = Z_{t=0}' / (S \cdot \cos \beta^\circ) = i_{t=0} (1 - \cos \beta^\circ) / \cos \beta^\circ$$

Accordingly, formulas (21)–(23) can be expressed as:

$$i_{t=0}^s = i_{t=0} + i_{t=0}' = i_{t=0} (1 / \cos \beta^\circ) \quad (26)$$

$$P_{t=0} = i_{t=0} \cdot X \cdot Y (1 - n_1/n) = i_{t=0} \cdot X \cdot Y (1 - \cos \beta^\circ) \quad (27)$$

$$\begin{aligned} P_{t=0}' &= i_{t=0}' \cdot X \cdot Y (n_1/n) = i_{t=0}' (1 - \cos \beta^\circ) / \cos \beta^\circ \cdot X \cdot Y (n_1/n) \\ &= i_{t=0} \cdot X \cdot Y (1 - \cos \beta^\circ) \end{aligned} \quad (28)$$

From the two formulas (27) and (28), $P_{t=0} = P_{t=0}'$ follows. This means, if the dimensions X , Y and Z in the old and the new models are the same, the material consumption due to the possible increase in the number of fins will not be higher. That also means that by non-negligible fin thicknesses the number of fins and also the material consumption reduces. The saving in material consumption of fins can be calculated by the formula:

$$S_f = (i_{t=0}^s - i_{t=0}^s) / i_{t=0}^s \cdot 100\% \quad (29)$$

5. Numerical investigation of the model developed

5.1. Organization of the simulation investigations

To verify the formulas set up, two cases for designing two models with different numbers of tube rows will be tested. For this,

the same boundary conditions as in the previously studied cases will be used.

To simplify the investigations, just the segment that is located on the straight section of the tube is examined. The one on the curved section will remain unattended. It is expected to get a little smaller heat transfer value on the curved section than on the straight section. This is due to the decrease in the contact area between fins and tubes while this contact area changes its shape from elliptical at straight sections to round shape at the top of the curvature. However, the curved section is much smaller than the straight one and in this work it will not be investigated.

It should be noted that the air direction remains perpendicular to entry surfaces. The obtained heat transfer and loss power values for two cases are compared with each other as well as with those in the old model, which consists of four tube rows without inclination of the tubes or fins. The following tests will analyze the cases of $n_1 = 3$ and $n_1 = 2$.

5.1.1. Test case 1

The number of tube rows is reduced from 4 to 3 in the new model. Based on the formula developed (17), we can calculate the angle of elbow of the tubes $2\alpha^\circ = 97.18^\circ$, which leads to the fact that the tubes are bent at an angle of $\beta^\circ = 41.41^\circ$. Therefore, the height of the fins is reduced. The new fin height is:

$$H = A + B + 3D + 2C \approx 132.5 \cdot \cos 41.41^\circ = 99.374 \text{ mm.}$$

The total fin number in the new model can be calculated by using formula (21):

$$i_t^{s1} = 979 \text{ fins}$$

According to formula (29) we can calculate the savings in fin material directly:

$$S_{f1} = (1000 - 979) / 1000 \cdot 100 \approx 2.1\%$$

5.1.2. Test case 2

In this test case, the height of the fins is reduced by removing their two upper parts through reducing the number of tube rows from 4 to 2. According to formula (17), we can calculate the angles $2\alpha^\circ = \beta^\circ = 60^\circ$. In this case, the fin height is reduced by half $H = 66.25$ mm. As the number of fins depends on the inclined tube angle, their number can be increased to:

$$i_t^{s2} = 1409 \text{ fins}$$

In this case, the savings in fin material can be calculated by using the formula (29):

$$S_{f2} = (1500 - 1409) / 1500 \cdot 100 \approx 6\%$$

5.2. Results and discussion

Assuming that the length of the tubes is constant in both test cases, the cell number along the tubes is calculated by using formulas (14) and (15). Taking into consideration the angle of curvature of the tube we can calculate the number of elbows. We note that the tubes at both sides of the model are bent at another angle ($180^\circ - \beta^\circ$). For instance, when the angle β° is 41.41° , the heat exchanger consists of 28 elbows with angle $2\alpha^\circ = 97.18^\circ$ and 6 elbows with angle 138.59° at the sides of the heat exchanger (two side elbows per tube row).

As mentioned above, the air entrance area in both models is not changed. The distance S will be kept constant but the new distance between two fins decreases to ($S \cdot \sin \omega^\circ = S \cdot \cos \beta^\circ$). Table 4

Table 4
The main calculated data for designing a new model in two cases compared with the data of the old model.

model	β°	$2\alpha^\circ$	n	n_1	K	L	M	e	Length of the four tubes ^a	Number/Angle of elbows	Number of fins
Old model	0	0	4	4	–	–	–	–	6428	–	750
Test case 1	41.41	97.18	4	3	24.75	37.42	56.12	29	6428	28/(97.18°) 6/(138.59°)	979
Test case 2	60	60	4	2	98.99	114.32	114.32	14	6428	13/(60°) 4/(120°)	1409

^a A tube length is almost equal to the heat exchanger length or the sum of fin thicknesses and the distances between them. This value (6428 mm) was calculated for four staggered tubes.

shows all the dimensions required for designing the new model in both cases and, in addition, the data for calculating the pressure drop in the tubes.

Simulations are carried out in both cases to get the heat transfer values on the fins and tube surfaces, and the pressure loss in each case is calculated which determines the required fan power.

The pressure loss within the tubes increases because of the friction losses in the tube walls and, in addition, losses occur through the deflection of the tubes and may be expressed as:

$$\Delta p = \Delta p_1 + \Delta p_2 \tag{30}$$

Here, Δp_1 , Δp_2 are the pressure drop through the tube wall and the pressure drop through the elbows, respectively. They are given by (cf. [23]):

$$\Delta p_1 = \zeta_1 \cdot L/d_i \cdot \rho \cdot u^2/2 \tag{31}$$

$$\Delta p_2 = \zeta_2 \cdot \rho \cdot u^2/2 \tag{32}$$

where: ζ_1 : pressure loss coefficient through friction in the tube wall
 ζ_2 : pressure loss coefficient of the elbows ρ , u : density and velocity, resp., along the flow path L : total length of the tube d_i : internal diameter of the tube

In general, the pressure loss coefficient ζ_1 depends on the Reynolds number Re_i of the fluid flow inside the tubes, which can be given within the range from $Re_i \approx 2 \cdot 10^4$ to $Re_i \approx 2 \cdot 10^6$ by the simple formula (cf. [23]):

$$\zeta_1 = 0.00540 + 0.3964/Re_i^{0.3} \tag{33}$$

According to the elbow angle and Reynolds number, the pressure loss coefficient ζ_2 can be calculated approximately using Fig. 8

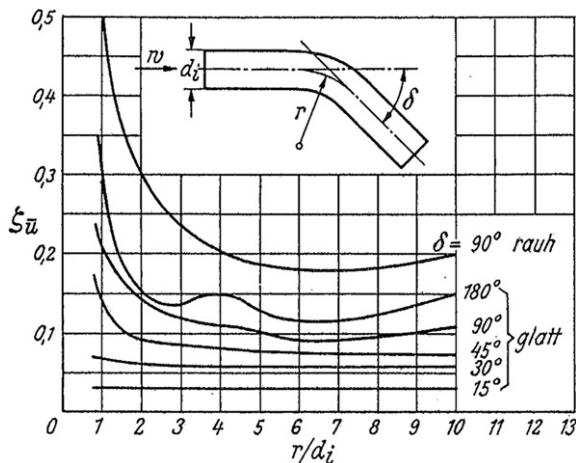


Fig. 8. Pressure loss coefficient ζ_2 of the elbows with $Re_i > 10^5$ from Ref. [23].

(The figure is taken from Ref. [23]). The heat transfer values and the calculated loss power are presented in Table 5. Furthermore, the heat transfer and the loss power values of the old model are provided for the purpose of comparison with the values obtained for two cases with the new model. Fig. 9 shows the temperature distribution on the surfaces of the fins in the first and second test cases.

Considering Table 5, we see that, in comparison to the old model, the heat transfer increased considerably by 28.20% in the first test case and by 59.13% in the second test case.

$$\dot{Q} = \dot{V} \cdot \rho \cdot c_p \cdot \Delta T; \quad \dot{V} = u \cdot A \tag{34}$$

According to the equation (34) (cf. [20]) a significant augmentation of the heat transfer returns on the one hand to increasing the velocity of the air between the two adjacent fins. This is the result of decreasing the distances between two adjacent fins since the volumetric (\dot{V}) flow rate along the heat exchanger should remain constant. On the other hand, the angle between the fins and tubes which will result in an elliptical shape of the contact line will reduce the wake region behind the tubes. Furthermore, the turbulence in the developed design is increased due to the change in the direction of air flow between the fins. These will in turn increase the amount of heat transfer.

In order to keep the volume flow between the fins constant, the fan power was increased by enhancing the number of fins and the decrease of the distances between adjacent fins from 5.48 W in the old model to 17.23 W in test case 1 and to 45 W in test case 2. In case 2, the required fan power is greater than in case 1 because of a larger number of fins in case 2 and, thus, the cross-sections between the fins are smaller. Conversely, the pressure loss in the tubes¹ increased more in case 1 than in case 2, which is due to the fact that, in case 1, the number of elbows is higher than in case 2. The normalized values of the total power consumption were increased to 277% of 6.79 W in the first case and to 685% in the second case. The increase in the heat transfer amounted to 128% of 759.7 W in the first case and to 159.13%, which equals an increase of 214.25 W and 449.25 W in the two cases, respectively. To underline the efficiency of the new model and to compare these two cases with the old model more precisely we calculated the ratio between the total power consumption (\dot{Q}_{con}) and the amount of heat transfer obtained (\dot{Q}). This ratio was increased from 0.8% in the old model to 1.93% in the case 1 and to 3.84% in the case 2 as illustrated in Table 5.

The amount of fin materials used for the construction of the heat exchanger can be reduced by reducing the fin height. Furthermore, the modification of the contact line between the tubes and the fins from a round into an elliptical shape leads to an enlargement of the contact surface between the fins and the tubes. This elliptical

¹ These calculated values are carried out without considering the tube sections, which are outside of the heat exchanger.

Table 5
Comparison of the new models with the old model.

Model	Heat transfer rate $\dot{Q} = \dot{Q}_1 + \dot{Q}_2$ (W)	Heat transfer enhancement (W)	Normalized \dot{Q} (%)	Loss power due to pressure drop (Fan) (W)	Loss power due to pressure drop (water pump) $(\Delta p_1 + \Delta p_2) \cdot \dot{V} / \eta$ (W)	Total power consumption \dot{Q}_{con} (W)	Normalized \dot{Q}_{con} (%)	\dot{Q}_{con} / \dot{Q} (%)
Old model	$1.013 \cdot 750 = 759.75$	0	100	$0.0073 \cdot 750 = 5.48$	1.31	6.79	100	0.8
Test case 1	$0.995 \cdot 979 = 974$	214.25	128.20	$0.0176 \cdot 979 = 17.23$	1.60	18.83	277	1.93
Test case 2	$0.858 \cdot 1409 = 1209$	449.25	159.13	$0.032 \cdot 1409 = 45$	1.48	46.48	685	3.84

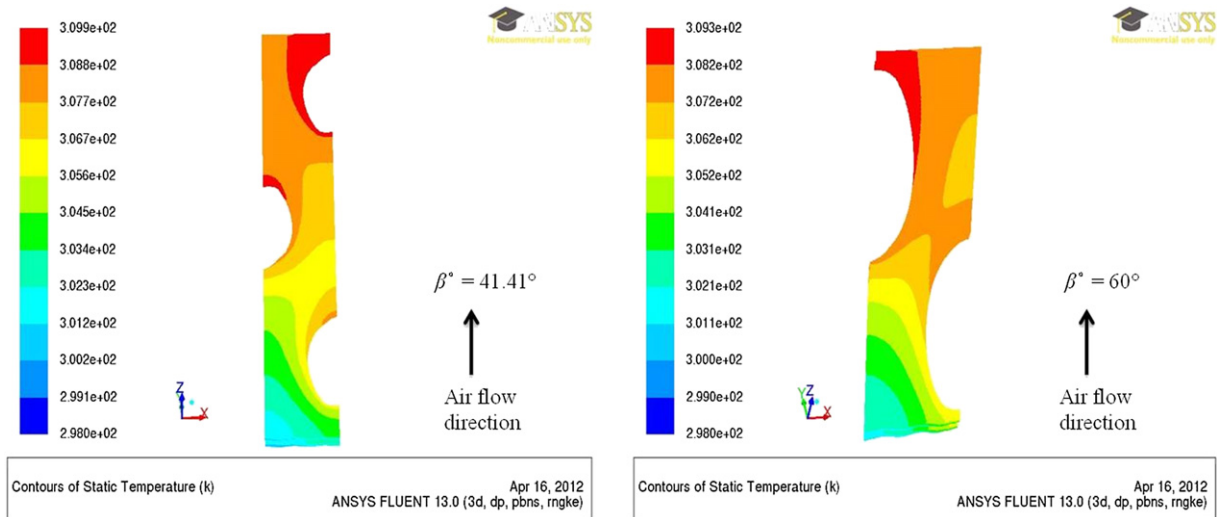


Fig. 9. Temperature distribution on the surfaces of the fins in new models.

contact line reduces the required amount of fin material. To compare the consumption of material between the old and the new model, we carry out the following calculation. First, we consider the heat transfer in the same segment investigated in the old and in the new models. Then, we multiply this value by a number of fins which will ensure a heat transfer of 759.75 W. This value is the maximum achievable heat transfer of the considered segments in the old model (see Table 5). The potential savings of fins and tube material consumption and of the areas required are shown in Table 6.

Analogous to formula (29), the saving in fin material can be calculated by using the following formula:

$$S_f = (i_{t=0}^s - i_{req}) / i_{t=0}^s \cdot 100\% \quad (35)$$

Since the fin thickness and the distance between the adjacent fins are constant, and the tubes form symmetrical cells as well, the saving in material consumption of the tubes and the saving in the

required area for the heat exchanger can be calculated depending on the number of fins (i_t^s, i_{req}) by means of the formula:

$$S = (i_t^s - i_{req}) / i_t^s \cdot 100\% \quad (36)$$

As it can be seen in Table 6 the realization of the same amount of heat transfer of the old model in the new models, results in saving in the material consumption of the fins and tubes and therefore the required area for the heat exchanger.

The amount of fins material saving in the first case is 23.96%, and it amounts to 40.90% in the second case. As a result, the saving in tubes material and in the required area for the heat exchanger is 21.96% in the first case, because one of the tube rows is removed, and 37.12% in the second case due to the removal of two tube rows. Moreover, there is some material saving due to the reduction in the number of tube windings outside the heat exchanger which is in turn due to the reduction in the number of the tube rows. We did not calculate the exact amount of this saving, so it is not included in these numbers. Furthermore, the required water pump power in

Table 6
Comparison of the material consumption between the old and the new models at constant heat transfer rate.

Model	Heat transfer rate $\dot{Q} = \dot{Q}_1 + \dot{Q}_2$ (W)	Required number of fins i_{req}	Saving in material consumption of fins S_f /tubes, and in required area for the heat exchanger S (%)	Loss power due to pressure drop (fan) (W)	Loss power due to pressure drop (water pump) (W)	Total power consumption \dot{Q}_{con} (W)	Normalized \dot{Q}_{con} (%)	\dot{Q}_{con} / \dot{Q} (%)
Old model	759.75	750	0.0	$0.0073 \cdot 750 = 5.48$	1.31	6.79	100	0.8
Test case 1	759.75	764	23.96/21.96	$0.0176 \cdot 764 = 13.45$	1.28	14.73	216.94	1.9
Test case 2	759.75	886	40.90/37.12	$0.032 \cdot 886 = 28.35$	0.94	29.29	431.37	3.9

the new models was decreased by decreasing the overall tube length. The ratio (\dot{Q}_{con}/\dot{Q}) is 1.9% in test case 1 and 3.9% in test case 2.

However, the investigations carried out did not aim to find the optimal solution but to describe a method for designing an effective heat exchanger by the reconfiguration of a zigzag shape and to illustrate the benefits of this new design too, whereas we can carry out various options to develop the model. For example, the effect of changing the parameters of α° , ω° , K , M , L , Z or Y can be investigated.

One may think that the proposed design is difficult to manufacture, however, it offers some good advantages such as: an increase in the efficiency and a decrease in the number of tube rows as well as the number of tube windings outside the heat exchanger (to form a tube coil), thus leading to a decrease in material consumption and space required. Therefore, investments in this design would be worth.

6. Summary and conclusions

A new method has been developed for designing effective heat exchangers. The new models were analyzed by simulation with the aim to determine the resulting heat transfer and pressure drop in order to illustrate the advantages and disadvantages of the new design. Two design alternatives were examined in detail. In the first case, the number of tube rows was reduced from 4 to 3 and the fin height by 25%. In the second case, the number of tube rows was reduced from 4 to 2 and the fin height by 50%.

Due to the decrease of the fin heights, the number of fins in the respective model could be increased. Furthermore, more alternatives were presented to optimize the models investigated. The simulation results were analyzed and presented comprehensively. The conclusions can be summarized as follows:

- The new arrangement of the fins and the tubes in the model developed was implemented without increasing the material consumption.
- New formulas were developed for designing an effective heat exchanger.
- A significant increase in heat transfer was achieved due to the increase of the effective areas of the fins.
- Furthermore, the increase in heat transfer resulted mainly from the elliptical contact between fins and tubes, an increase in air velocity and turbulence.
- An increase in the fan power was realized to ensure the same volume flows between the added fins, and to compensate the increase in the pressure drop.
- For the first case, the overall heat transfer improvement achieved, determined in a segment of sixty to 979 fins, and the normalized value were 214.25 W and 128.20%, resp. The total power consumption was 18.83 W and it equates 1.9% from the heat transfer gained.
- For the second case, the overall heat transfer improvement achieved, determined in a segment of sixty to 1409 fins, and the normalized value were 449.25 W and 159.13%, resp. The total power consumption was 46.48 W and it equates 3.9% from the gained heat transfer.
- Very low increase in the pump power because of the arc or elbow pieces. The required pump power was 1.60 in the first case and 1.48 W in the second one. Designing heat exchangers by means of the method presented can reduce their dimensions significantly without reducing heat transfer.
- The increase of total power consumption was small in the new model in both cases compared with the heat transfer gained.
- Designing a heat exchanger by means of the method proposed, in order to achieve the same heat transfer as in the existing

type can reduce their dimensions significantly. The saving in material consumption of the fins reaches 23.69% and 40.93% in the first and second case, resp. The saving in material consumption for tubes and the required area for the heat exchanger reaches 21.96% and 37.12%, in the first and second case, resp.

Acknowledgements

The authors are grateful to the Ilmenau University of Technology for their support in this study.

References

- [1] S. Kaminski, U. Groß, Air-side heat transfer and pressure drop in finned tube heat exchangers (Luftseitiger Wärmeübergang und Druckverlust in Lamellenrohr-Wärmeübertragern), *Kl. Luft- und Kältetechnik* 1 (2000) 13–18 (in German).
- [2] R. István, Numerical study of the air-side heat transfer and pressure drop in finned-tube heat exchangers with different tube forms (Numerische Untersuchung des Luftseitigen Wärmeübergangs und Druckverlustes in Lamellenrohr-Wärmeübertragern mit verschiedenen Rohrformen), Thesis, Freiberg, Germany, 2004 (in German).
- [3] C.W. Lu, J.M. Huang, W.C. Nien, C.C. Wang, A numerical investigation of the geometric effects on the performance of plate finned-tube heat exchanger, *Energy Conversion and Management* 52 (3) (2011) 1638–1643.
- [4] S. Kaminski, Numerical simulation of air-side flow and heat transfer processes in finned tube heat exchangers (Numerische Simulation der luftseitigen Strömungs- und Wärmetransportvorgänge in Lamellenrohr-Wärmeübertragern), Thesis, Freiberg, Germany, 2001.
- [5] R. Remero-Méndez, M. Sen, K.T. Yang, R. McClain, Effect of fin spacing on convection in a plate fin and tube heat exchanger, *International Journal of Heat and Mass Transfer* 43 (2000) 39–51.
- [6] Y.C. Liu, S. Wongwises, W.J. Chang, C.C. Wang, Airside performance of fin-and-tube heat exchangers in dehumidifying conditions – data with larger diameter, *International Journal of Heat and Mass Transfer* 53 (7–8) (2010) 1603–1608.
- [7] Y. Kim, J. Kim, D. Sin, Effects of fin and tube alignment on the heat transfer performance of finned-tube heat exchangers with large fin pitch, in: *International Refrigeration and Air Conditioning, Conference Paper*, vol. 716, 2004.
- [8] M. Abu Madi, R.A. Johns, M.R. Heikal, Performance characteristics correlation for round tube and plate finned heat exchangers, *International Journal of Refrigeration* 21 (7) (1998) 507–517.
- [9] Y.C. Tsai, J.Y. Jang, Optimization analysis for louver fin heat exchangers, in: *2nd International Congress on Computer Applications and Computational Science Advances in Intelligent and Soft Computing*, vol. 144, 2012, pp. 477–482.
- [10] A.B. Ganorkar, V.M. Kriplani, Review of heat transfer enhancement in different types of extended surfaces, *International Journal of Engineering Science and Technology (IJEST)* 3 (4) (2011) 3304–3313.
- [11] F. Ghiani, flat tube heat exchanger as well as heat exchange tube (Wärmetauscher sowie Wärmetauschrohr), DE patent 10 2008 020 230 A1. 2008 October 30 (in German).
- [12] K.M.K. Pasha, Heat transfer and pressure drop investigation for a bank of inclined flat tubes, *Journal of American Science* 8 (8) (2012) 351–356.
- [13] H.M. Sahin, A.R. Dal, E. Baysal, 3-D numerical study on the correlation between variable inclined fin angles and thermal behavior in plate fin-tube heat exchanger, *Applied Thermal Engineering* 27 (2007) 1806–1816.
- [14] D. Karmo, S. Ajib, Study of the influences of the fins shape on the heat transfer properties of a dry cooling tower (Untersuchung der Einflüsse der Lamellenformen auf die Wärmeübertragungseigenschaften eines Trockenkühlturms), In: *DKV-Conference, Aachen, Germany, 2011* (in German).
- [15] S. Ajib, W. Günther, Investigation results on dry cooling tower with finned-tube heat exchanger, in: *4th International Conference Solar Air-conditioning, Cyprus, Turkey, 2011*.
- [16] J.H. Ferziger, M. Peric, *Computational Methods for Fluid Dynamics*, third ed., Springer Reference, Berlin, Germany, 2002.
- [17] M.N. Özisik, *Heat Transfer a Basic Approach*, International, McGraw-Hill Book Company, 1985.
- [18] S. Kakac, Y. Yener, *Convective Heat Transfer*, second ed., CRC Press Begell House, Boca Raton, FL, 1995, pp. 279–309.
- [19] P. Sagaut, *Large Eddy Simulation for Incompressible Flows*, third ed., Berlin, Germany, 2005.
- [20] W. Polifke, J. Kopitz, *Heat Transfer (Wärmeübertragung)*, second ed. Pearson Education, Maschinenbau, Munich, Germany, 2009 pp. 332–343 [in German].
- [21] W. Wagner, *Heat Exchanger (Wärmeaustauscher)* fourth ed. (2009). Würzburg, Germany (in German).
- [22] C.N. Lin, Y.W. Liu, J.S. Leu, Heat transfer and fluid flow analysis for plate-fin and oval tube heat exchangers with vortex generators, *Heat Transfer Engineering* 29 (7) (2008) 588–596.
- [23] *VDI-heat Atlas, VDI Wärmeatlas, Berechnungsblätter für den Wärmeübergang, Druckverlust bei der Strömung durch Leitungen mit Querschnittsänderung*, vol. 9, Springer Reference, Berlin, 2002 (in German).